Nitrification in the euphotic zone as evidenced by nitrate dual isotopic composition: Observations from Monterey Bay, California

Scott D. Wankel,[1,2,3] Carol Kendall,[4] J. Timothy Pennington,[5] Francisco P. Chavez,[5] and Adina Paytan[1]

Received 19 March 2006; revised 4 December 2006; accepted 11 January 2007; published 4 May 2007.

[1] Coupled measurements of nitrate (NO_3^-), nitrogen (N), and oxygen (O) isotopic composition ($\delta^{15}N_{NO3}$ and $\delta^{18}O_{NO3}$) were made in surface waters of Monterey Bay to investigate multiple N cycling processes occurring within surface waters. Profiles collected throughout the year at three sites exhibit a wide range of values, suggesting simultaneous and variable influence of both phytoplankton NO_3^- assimilation and nitrification within the euphotic zone. Specifically, increases in $\delta^{18}O_{NO3}$ were consistently greater than those in $\delta^{15}N_{NO3}$. A coupled isotope steady state box model was used to estimate the amount of NO_3^- supplied by nitrification in surface waters relative to that supplied from deeper water. The model highlights the importance of the branching reaction during ammonium (NH_4^+) consumption, in which NH_4^+ either serves as a substrate for regenerated production or for nitrification. Our observations indicate that a previously unrecognized proportion of nitrate-based productivity, on average 15 to 27%, is supported by nitrification in surface waters and should not be considered new production. This work also highlights the need for a better understanding of isotope effects of NH_4^+ oxidation, NH_4^+ assimilation, and NO_3^- assimilation in marine environments.

Citation: Wankel, S. D., C. Kendall, J. T. Pennington, F. P. Chavez, and A. Paytan (2007), Nitrification in the euphotic zone as evidenced by nitrate dual isotopic composition: Observations from Monterey Bay, California, *Global Biogeochem. Cycles*, *21*, GB2009, doi:10.1029/2006GB002723.

1. Introduction

[2] Despite decades of research on marine nutrient dynamics, much remains to be learned about the marine nitrogen (N) cycle. Fluxes among pools of N and rates of transformation of N species are poorly characterized in the upper water column. In the euphotic zone, phytoplankton generally represent the largest pool of particulate organic nitrogen (PON) and the largest sink for inorganic N. As cells die, the organic biomass is remineralized by heterotrophic processes. The remineralized N is primarily released as ammonium (NH_4^+) which is either reassimilated by planktonic organisms or oxidized to nitrite (NO_2^-) and nitrate (NO_3^-) by nitrifying bacteria and/or archaea [*Karl and Michaels*, 2001; *Sigman and Casciotti*, 2001].

[3] Primary production by phytoplankton in ocean surface waters is chiefly regulated by the availability of nitrogenous nutrients (NH_4^+ and NO_3^-). Hence upwelling of NO_3^- rich, deep water often results in high primary production. Production in surface water is additionally driven by NH_4^+ generated from the remineralization of organic N. Many studies have estimated production of 'new' organic matter supported by upwelling of 'new' NO_3^- into the euphotic zone in terms of "*f*-ratios" constructed from the uptake of NO_3^- and NH_4^+, (where $f = NO_3^-$ uptake/(NO_3^- + NH_4^+ uptake)) [*Dugdale and Goering*, 1967; *Eppley and Peterson*, 1979; *Kudela and Dugdale*, 2000]. However, the relative importance of NO_3^- from nitrification within the euphotic zone fueling 'recycled' production has not been directly estimated. Hence estimates of new and regenerated production based on NH_4^+ and NO_3^- uptake will be inaccurate to the extent that some NO_3^- is regenerated within surface waters. Indeed, several studies have shown evidence for simultaneous nitrification and assimilation by phytoplankton occurring in the euphotic zone [*Ward et al.*, 1989; *Dore and Karl*, 1996; *Bianchi et al.*, 1997; *Raimbault et al.*, 1999; *Ward*, 2005], and primary production based on surface-regenerated NO_3^- may be underrepresented in current models [e.g., *Sarmiento et al.*, 1993].

[4] While these N cycling processes are well characterized, in situ flux measurements remain difficult to determine particularly where concentrations are low (e.g., surface waters) and where simultaneous processes may interfere with rate measurements of any one process (e.g., remineralization, assimilation, nitrification). However, the isotopic

[1]Department of Geological and Environmental Sciences, Stanford University, Stanford, California, USA.
[2]Also at United States Geological Survey, Menlo Park, California, USA.
[3]Now at Department of Organismal and Evolutionary Biology, Harvard University, Cambridge, Massachusetts, USA.
[4]United States Geological Survey, Menlo Park, California, USA.
[5]Monterey Bay Aquarium Research Institute, Moss Landing, California, USA.

0886-6236/07/2006GB002723$12.00

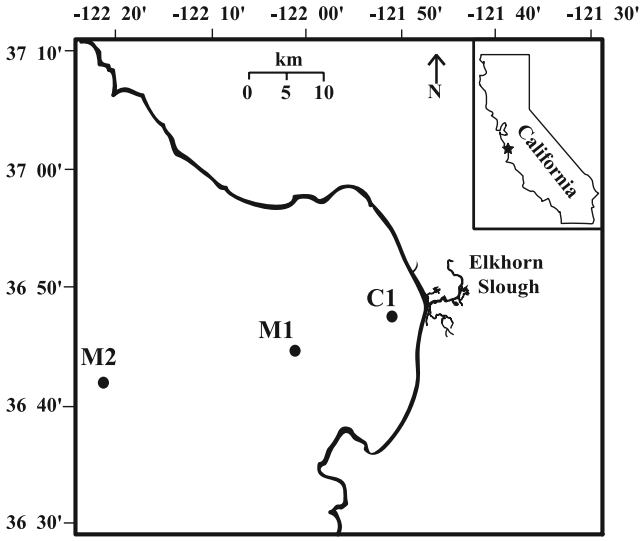

Figure 1. Map of Monterey Bay, California, showing sampling locations.

composition (e.g., $^{15}N/^{14}N$) of the various N pools has been shown to be a time/space-integrated record of multiple biogeochemical processes [e.g., *Brandes and Devol*, 2002; *Sigman et al.*, 2003]. Also, measurement of the natural abundance isotopic composition of the N pools avoids any undesired effects of ^{15}N labeling techniques which require sample manipulation and addition of exogenous nutrients. Furthermore, NO_3^- can be analyzed for both N ($\delta^{15}N_{NO3}$) and O ($\delta^{18}O_{NO3}$) isotopes helping to deconvolute some of the multiple processes occurring simultaneously within the water column [*Granger et al.*, 2004; *Lehmann et al.*, 2004; *Sigman et al.*, 2005].

[5] Any element containing multiple stable isotopes (e.g., ^{14}N and ^{15}N) is subject to some degree of mass-dependent isotopic fractionation due to the different rates at which each isotope reacts. For example, as a pool of NO_3^- is consumed by phytoplankton, the molecules containing the lighter isotopes (i.e., ^{14}N) react more quickly causing the $^{15}N/^{14}N$ ratio of the remaining NO_3^- to increase (higher $\delta^{15}N_{NO3}$ values). The magnitude of this effect is expressed as ε and is approximated as the difference between the $\delta^{15}N$ values of the substrate (e.g., NO_3^-) and that of the instantaneous product (e.g., $\delta^{15}N$ of phytoplankton). When two elements with stable isotopes are considered (e.g., N and O in NO_3^-), the fractionation can be viewed as "coupled" if the $\delta^{15}N$ and $\delta^{18}O$ shift proportionally in the same directions, and "decoupled" if not. Nitrate assimilation, for example, causes equal increases in $\delta^{15}N$ and $\delta^{18}O$ of the residual NO_3-; hence, the fractionations can be viewed as strongly coupled [*Granger et al.*, 2004]. Studies of NO_3^- isotopic fractionation in marine systems indicate that denitrification, like assimilation, also gives rise to $^{18}\varepsilon:^{15}\varepsilon = 1$ (e.g., coupled) [*Granger*, 2006]. Thus both NO_3^- assimilation and denitrification in marine environments yield similar ratios of O:N isotope fractionation and will result in an expected slope of 1 on a plot of $\delta^{15}N_{NO3}$ and $\delta^{18}O_{NO3}$.

[6] Unlike the NO_3^- consuming processes described above, nitrification (oxidation of NH_4^+ to NO_2^- and NO_3^-) leads to a decoupling of N and O isotope fractionations. Ammonium, the ultimate source of N to the NO_3^- molecule in this process, has been shown to be strongly fractionated during nitrification, with marine nitrifiers exhibiting values for ε_{ntr} between 14 and 19‰ [*Casciotti et al.*, 2003]. Thus the process of nitrification is potentially a source of NO_3^- with isotopically light N. The degree of fractionation, however, depends on several factors including the degree of consumption and the presence of other processes competing for the same NH_4^+ substrate (see model description).

[7] The $\delta^{18}O$ resulting from nitrification ($\delta^{18}O_{ntr}$), on the other hand, is the subject of some continuing debate. Biochemical studies have shown that the oxygen atoms of NO_3^- formed during nitrification are derived from both water and dissolved O_2 [*Andersson and Hooper*, 1983; *Kumar et al.*, 1983; *Hollocher*, 1984]. However, *Casciotti et al.* [2002] showed that in the marine water column, the $\delta^{18}O_{NO3}$ in deep waters is only slightly higher than the $\delta^{18}O$ of seawater and suggested that, owing to nitrite-water exchange [*Andersson et al.*, 1982], less than 1/6 of the oxygen atoms in NO_3^- originate from dissolved O_2. Thus formation of new NO_3^- from NH_4^+ through nitrification may result in a $\delta^{18}O$ approaching that of the ambient water [*Wankel et al.*, 2006]. In fact, there is increasing evidence that in the deep ocean, NO_3^- has a $\delta^{18}O_{NO3}$ consistently 2–3‰ higher than seawater (~0‰) [*Casciotti et al.*, 2002; *Sigman et al.*, 2005]. On the basis of these studies, we assume that the $\delta^{18}O_{NO3}$ resulting from nitrification in the surface ocean operates in the same manner, returning NO_3^- with a $\delta^{18}O_{NO3}$ of ~3‰.

[8] The decoupling of O and N fractionation in the N cycle allows for the dual isotope approach to help deconvolute multiple processes. For example, deviations from $^{18}\varepsilon:^{15}\varepsilon = 1$ can arise from the combined effects of N fixation and removal by denitrification [*Sigman et al.*, 2005]. Near the surface, the combined processes of assimilation and nitrification should also cause similar deviations from the $\delta^{15}N_{NO3}$ and $\delta^{18}O_{NO3}$ relationship expected from assimilation alone. This has been pointed out by others [*Granger et al.*, 2004; *Sigman et al.*, 2005]. Specifically, if supply of NO_3^- from deep water and consumption by NO_3^- assimilation are the only processes occurring in the euphotic zone, changes in $\delta^{15}N_{NO3}$ should parallel those of $\delta^{18}O_{NO3}$. However, our study in Monterey Bay shows a decoupling of the $\delta^{15}N$ and $\delta^{18}O$ of NO_3^-, indicating other processes are important in the euphotic zone marine N cycle. By taking into account parallel variations in both the $\delta^{15}N_{NO3}$ and $\delta^{18}O_{NO3}$, we estimate the relative amount of primary production supported by euphotic zone nitrification in an area dominated by delivery of nutrients through upwelling.

2. Site Description

[9] Monterey Bay is a broadly open and deep nonestuarine embayment (>1000 m) on the central coast of California (Figure 1). It is characterized by large spatial and temporal changes in productivity due to seasonal changes in the strength of upwelling-favorable northwesterly winds. During the spring and early summer, increased wind stress leads to upwelling of nutrient-rich water, resulting in higher

productivity. During the fall and winter months, these winds relax or reverse, causing a cessation of upwelling leading to lower productivity. Sea surface temperatures range from 9°C during upwelling events to >16°C in late summer [*Breaker and Broenkow*, 1994; *Chavez*, 1995, 1996; *Pennington and Chavez*, 2000]. Oceanographic conditions during winter are spatially more uniform, with relatively low levels of NO_3^- (~1 μM), chlorophyll (~1 μg/L), and primary productivity (<500 mg C/m^2). As northwesterly winds increase in spring, spatial and temporal variability in all of these parameters increases due to the episodic and localized nature of the strong winds and upwelling events. High concentrations of NO_3^- are common (~30 μM), and during blooms of phytoplankton chlorophyll concentrations can reach 20 μg/L [*Kudela and Chavez*, 2002]. Phytoplankton dynamics and nutrient addition experiments suggest that the system is largely NO_3^- driven, with little evidence for N fixation [*Pennington and Chavez*, 2000; *Kudela and Chavez*, 2002]. Following the upwelling season, there is a period (late summer to early fall) during which more open oceanic conditions prevail. Hence Monterey Bay provides an excellent opportunity to assess the influence of variations in NO_3^- isotopic composition on estimates of euphotic zone nitrification in a highly dynamic region.

[10] Three long-term oceanographic observational stations (C1, M1, and M2) are located in Monterey Bay. C1 is closest to shore (36°47.8′N, 121°50.8′W) and is most influenced by coastal and within-bay processes (Figure 1). Station M1 (36°44.7′N, 122°01.2′W) is situated directly downstream of a major upwelling current and thus responds directly to upwelling events. Station M2 (36°41.9′N, 122°23.9′W) is the most oceanic of the stations and generally is less influenced by seasonal upwelling. Euphotic zone depths typically range from 30 to 60 m, while mixed layer depths are generally somewhat shallower (10 to 40 m).

3. Methods: Sample Collection

[11] Samples were collected during nine single-day cruises between November 2002 and June 2004 aboard the R/V *Point Lobos* along an offshore transect comprising three stations (C1, M1 and M2). Owing to seasonally rough seas, the outermost station, M2, was visited fewer times in this study than C1 and M1. Casts were made to 200 m using a SeaBird 911 CTD mounted on a General Oceanics 12 sample rosette of 12L Niskin bottles. The suite of measurements made at each station is described in detail by *Pennington and Chavez* [2000]. Water was collected from 11 depths between 0 to 200 m. Ten milliliters of water from each depth was frozen and later analyzed for dissolved nutrient concentrations using an AlpChem autoanalyzer [*Pennington and Chavez*, 2000]. Fifty milliliters of water was collected, filtered (0.2 μm) and frozen for NO_3^- isotope measurements. Within this depth range, waters were always oxic, eliminating the possibility of influence by denitrification.

[12] Isotopic analyses of NO_3^- were carried out using the denitrifier method [*Sigman et al.*, 2001; *Casciotti et al.*, 2002]. All samples were corrected for exchange, fractionation and blanks using international NO_3^- standards USGS 34 and USGS 35 [*Böhlke et al.*, 2003]. Analytical precision (1σ) for an internal quality control NO_3^- standard was 0.3‰ for $\delta^{15}N_{NO3}$ and 0.8‰ for $\delta^{18}O_{NO3}$. Reproducibility of replicates (~65% of the samples were analyzed in duplicate) was slightly higher than this ($\delta^{15}N$ = 0.4‰; $\delta^{18}O$ = 0.9‰). $\delta^{15}N$ values are reported as $[(^{15}N/^{14}N_{sample})/(^{15}N/^{14}N_{ref}) - 1]*1000$, referenced to Air N_2. $\delta^{18}O$ values are reported as $[(^{18}O/^{16}O_{sample})/(^{18}O/^{16}O_{ref}) - 1] *1000$, referenced to VSMOW.

[13] The denitrifier method implicitly measures the isotopic composition of NO_3^- + NO_2^-. However, the potential contribution of NO_2^- is considered to be minor and the sum is reported as NO_3^-. If NO_2^- is abundant, the reported isotopic composition of NO_3^- may be inaccurate. The magnitude of this error will depend on the NO_2^- concentration in the sample as well as both the isotopic composition of the NO_2^- and the isotope effect for NO_3^- reduction to NO_2^- in the denitrifier species used, which is currently unknown. In order to minimize the interference of NO_2^- in our samples, data were not included if the relative amount of NO_2^- in the total oxidized N pool (NO_2^- + NO_3^-) was more than 4%. This occurred in surface waters on two different sampling dates (18 November 2003 and 21 January 2004) at all three sites, where NO_2^- accounted for 6 to 22% of the total oxidized N pool.

4. Results: $\delta^{15}N_{NO3}$ and $\delta^{18}O_{NO3}$

[14] Concentrations of NO_3^- in the upper 200 m ranged from 37.4μM to 0.7μM (Figures 2a, 2b, and 2c), with the lowest concentrations near the surface at all three stations, consistent with drawdown of NO_3^- by phytoplankton within the euphotic zone. Values for $\delta^{15}N_{NO3}$ ranged from +2.5‰ (M2, 17 September 2003) to +14.5‰ (M2, 6 March 2003), while $\delta^{18}O_{NO3}$ ranged from +1.1‰ (M1, 26 November 2002) to +33.9‰ (M2, 17 September 2003). Figure 2 shows depth profiles of $\delta^{15}N_{NO3}$ and $\delta^{18}O_{NO3}$ for each station. Both $\delta^{15}N_{NO3}$ and $\delta^{18}O_{NO3}$ values are typically higher in the euphotic zone as is expected from phytoplankton uptake. Because assimilative uptake has been shown to fractionate both N and O isotopes equally [*Granger et al.*, 2004], we expect equal increases in $\delta^{15}N_{NO3}$ and $\delta^{18}O_{NO3}$ relative to the composition in subsurface waters (e.g., a 1:1 slope originating at the composition of upwelled NO_3^-). However, in all profiles, $\delta^{18}O_{NO3}$ values exhibited larger relative increases than $\delta^{15}N_{NO3}$ values. This trend is shown in Figures 2j, 2k, and 2l, where we plot this deviation (see discussion about Δ(15,18) below). Thus NO_3^- isotopic composition in the euphotic zone does not appear to adhere to this simple $^{15}\varepsilon = {}^{18}\varepsilon$ rule associated with NO_3^- assimilation and suggests that it is recording multiple processes simultaneously.

4.1. Spatial and Temporal Variability

[15] During seasonal upwelling in Monterey Bay, concentrations of NO_3^- are variable. Early during an upwelling event, the concentrations are high in surface waters, followed by phytoplankton blooms which draw concentrations down. While upwelling is well-documented in Monterey Bay and evident in the NO_3^- concentration profiles (27 March 2003, 24 June 2003, 24 May 2004, 15 June 2004;

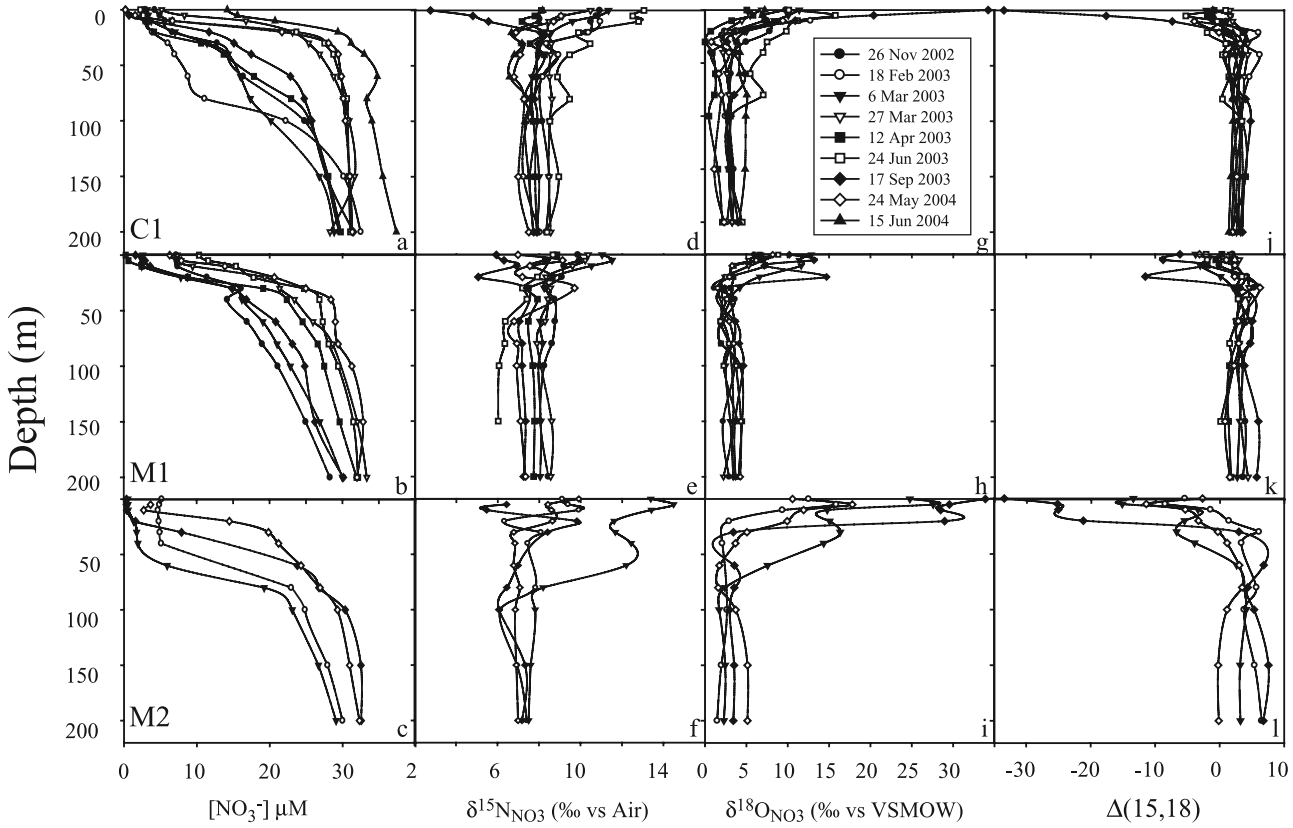

Figure 2. Depth profiles at stations C1, M1, and M2, respectively, of (a, b, c) NO_3^- concentrations, (d, e, f) $\delta^{15}N_{NO3}$, (g, h, i) $\delta^{18}O_{NO3}$, and (j, k l) $\Delta(15,18)$. Values for $\Delta(15,18)$ are referenced to mean North Pacific deep water nitrate ($\delta^{15}N = +5‰$; $\delta^{18}O = +3‰$).

Figure 2), no obvious seasonal patterns were evident in the profiles of NO_3^- isotopic composition. This may not be surprising in light of recent findings on nitrification dynamics in Monterey Bay in which *Ward* [2005] showed that bacterial abundance (potential mediators of remineralization), rates of NH_4^+ oxidation (a source of NO_3^-) and NH_4^+ assimilation by phytoplankton, are uncorrelated with a wide array of hydrological and biogeochemical parameters. Furthermore, the maximum rate of NH_4^+ oxidation was also unrelated to seasonal hydrographic or biogeochemical signals implying a decoupling of the N cycle from seasonal hydrographic features. Other researchers have also concluded that the links among upwelling, $\delta^{15}N_{NO3}$, $\delta^{15}N_{pon}$ and export flux are less tightly correlated in Monterey Bay than in the open ocean, most likely as the result of the smaller temporal and spatial scales of upwelling events [*Altabet et al.*, 1999].

[16] In the one sampling date during the oceanic period of our study (17 September 2003), $\delta^{15}N_{NO3}$ values in the surface water at all stations were actually lower than in deeper water. A common interpretation of low $\delta^{15}N_{NO3}$ values in surface water is inputs by N fixation. While this interpretation cannot be ruled out, there has been little historical evidence that N fixation plays an important role in Monterey Bay. Furthermore, these lower $\delta^{15}N_{NO3}$ values were typically associated with very high $\delta^{18}O_{NO3}$ values, which seems inconsistent with N fixation, as the NO_3^- derived from N fixation should result in $\delta^{18}O_{NO3}$ values near +3‰ [*Sigman et al.*, 2005].

[17] While temporal trends in the isotopic composition at each site are relatively minor (or at least not revealed at the temporal resolution of this data set), there are some spatial differences. Overall variability in the deep water was minimal. However, stations C1 and M1 (Figures 2e and 2d) generally have higher $\delta^{15}N$ values at 200 m (+7.8‰ and +8.0‰) as compared with M2 (+7.2‰) (Figure 2f). Near the surface, M2 also exhibits more variability and higher $\delta^{18}O$ values as compared to C1 and M1 (Figures 2g, 2h, and 2i), likely related to the lower NO_3^- concentrations, the higher degree of NO_3^- drawdown and the more stratified nature of this offshore site.

4.2. Decoupling of $\delta^{15}N_{NO3}$ and $\delta^{18}O_{NO3}$

[18] *Sigman et al.* [2005] define a term for the deviation of the N and O isotopic composition of NO_3^- from the 1:1 pattern expected from NO_3^- consumption (equation (1)). Such deviations may be observed when NO_3^- consumption is combined with production (nitrification),

$$\Delta(15,18) = \left(\delta^{15}N_{measured} - \delta^{15}N_{source}\right) - \left({}^{15}\varepsilon_p/{}^{18}\varepsilon_p\right) * \left(\delta^{18}O_{measured} - \delta^{18}O_{source}\right), \quad (1)$$

where $\delta^{15}N$ and $\delta^{18}O$ are the N and O isotopic composition of NO_3^- measured in the water parcel of interest and source water, respectively, and ${}^{15}\varepsilon_p$ (or ${}^{18}\varepsilon_p$) is the isotope effect for phytoplankton assimilation. This term, $\Delta(15,18)$ is equal to the horizontal deviation from a line with a slope of ${}^{18}\varepsilon:{}^{15}\varepsilon$

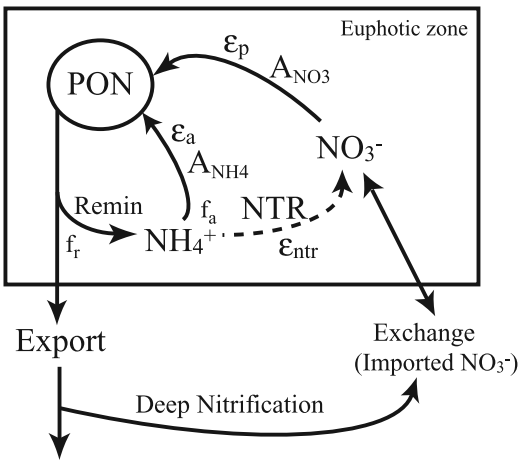

Figure 3. Schematic of steady state euphotic zone box model of NO_3^- isotopic composition. A_{NO3} refers to assimilation of NO_3^- by phytoplankton in the euphotic zone, with isotope effect ε_p. PON refers to the standing stock of particulate organic nitrogen in the surface water. Remin refers to the heterotrophic process of remineralization of sinking PON to NH_4^+, with f_r being the fraction of sinking PON that is remineralized rather than exported (Export). A_{NH4} refers to the reassimilation of NH_4^+ by phytoplankton, with isotope effect ε_a, while f_a is the fraction of NH_4^+ produced that is reassimilated (rather than oxidized). NTR refers to the oxidation of NH_4^+ (nitrification), with a isotope effect of ε_{ntr}. Exchange refers to the advective and/or diffusive flux of water and NO_3^- into and out of the box.

(in this case equal to 1) originating at some reference value (in this case, deep, upwelled NO_3^-) on a plot of $\delta^{15}N_{NO3}$ versus $\delta^{18}O_{NO3}$. While this term was originally used in zones of denitrification for evaluating N fixation, we adapt this term for use in surface waters to evaluate the presence of nitrification in the presence of assimilation [*Granger et al.*, 2004]. To investigate the impact of nitrification on $\delta^{15}N_{NO3}$ and $\delta^{18}O_{NO3}$, we construct a model detailed below and compare the observed data to model results.

5. Simple Steady State Box Model

[19] We present a simple steady state box model (Figure 3) of the surface ocean to help explore the combined effects of assimilation and nitrification on NO_3^- isotopic composition. The box model (Figure 3) was constructed on the basis of the following assumptions (see auxiliary materials[1] for model equation derivations):

[20] 1. External NO_3^- is supplied from upwelling of subeuphotic zone water and consumed by phytoplankton (PON) in the euphotic zone. Nitrate assimilation (A_{NO3}) is entirely by phytoplankton and the isotope effect (ε_p) for ^{15}N is equal to that of ^{18}O ($^{18}\varepsilon_p = {}^{15}\varepsilon_p$) [*Granger et al.*, 2004].

[21] 2. Nitrification resupplies NO_3^- within the euphotic zone having a $\delta^{15}N$ equal to $\delta^{15}N_{NH4} - \varepsilon_{ntr}$, where ε_{ntr} is the isotope effect for nitrification. On the basis of the calibration of the $\delta^{18}O$ of international NO_3^- isotope standards [*Böhlke et al.*, 2003], which adopts +25.6‰ for $\delta^{18}O_{NO3}$ of IAEA N3, the value for deep oceanic NO_3^- is thought to be near +3‰ [*Casciotti et al.*, 2002; *Sigman et al.*, 2005]. From this, we assume that nitrification in the ocean produces NO_3^- having a constant $\delta^{18}O$ of $\sim$ +3‰.

[22] 3. The $\delta^{15}N$ of PON ($\delta^{15}N_{pon}$) in the surface water results from the combination of both NO_3^- and NH_4^+ assimilation. Assimilation of NH_4^+ (A_{NH4}) results in a $\delta^{15}N_{pon}$ equal to $\delta^{15}N_{NH4} - \varepsilon_a$ (where ε_a is the isotope effect for A_{NH4}), while A_{NO3} results in a $\delta^{15}N_{pon}$ equal to $\delta^{15}N_{NO3} - \varepsilon_p$.

[23] 4. Ultimately, PON is subject to one of two processes, with a portion of this N sinking out of the box (Export) while the remaining fraction (f_r) is remineralized (Remin) to NH_4^+.

[24] 5. Because ambient NH_4^+ concentrations are assumed to be near zero, a fraction of the NH_4^+ pool is assumed to be reassimilated by phytoplankton (f_a; supporting traditionally 'regenerated production') while the remainder is assumed to be nitrified and returned as a source of recycled NO_3^- within the euphotic zone. Along with the partitioning between these two pathways (f_a), the isotope effects for each of the two processes (ε_a and ε_{ntr}) also exert an important control on the $\delta^{15}N$ of the NH_4^+ available for nitrification. At the branching reaction for NH_4^+ consumption we assume that ε_{ntr} is larger than ε_a (see discussion) [*Cifuentes et al.*, 1989; *Hoch et al.*, 1992; *Pennock et al.*, 1996; *Waser et al.*, 1998; *Casciotti et al.*, 2003].

[25] 6. Inputs from N fixation and denitrification are considered negligible in Monterey Bay.

[26] 7. Exchange of surface water with subsurface water is not considered to contribute significantly to import or export of NH_4^+ or PON. Thus we assume that the NH_4^+ pool is so rapidly utilized in the upper water column that we can neglect transport. Additionally we assume that the only removal of PON is through sinking or remineralization.

[27] Because no actual rate measurements have been made, we do not attempt to quantify the absolute rates of remineralization, nitrification or assimilation, only the changes in relative magnitudes of these fluxes. Thus we can constrain a ratio of NO_3^- supplied by nitrification within the euphotic zone to total NO_3^- uptake, or in other words, quantify the relative importance of nitrification within the surface water.

5.1. Box Definitions

[28] For the purposes of this model, we define a surface box on the basis of the depth of the mixed layer (Table 1). The boundaries of the mixed layer ranged from the surface water sample down to the bottom of the mixed layer (15 m to 65 m based on temperature profiles; where the thermocline approximates the nitracline). The NO_3^- isotopic composition of the surface box is calculated on the basis of the depth-integrated isotopic compositions of samples measured within this depth range (Figure 2).

[29] The depth-integrated composition of the source water to the surface box was estimated using data from below the mixed layer depth down to 200 m (Figure 2 and Table 1).

[1] Auxiliary materials are available in the HTML. doi:10.1029/2006GB002723.

Table 1. Site Characteristics During Sampling Period and Depth-Integrated Surface and Subsurface NO_3 Concentration and Isotopic Composition[a]

				Subsurface			Surface				
Date	Site	Season	Mixed Layer Depth, m	NO_3^- μM	$\delta^{15}N$	$\delta^{18}O$	NO_3^- μM	$\delta^{15}N$	$\delta^{18}O$	$\Delta(15,18)$[b]	f_n
11/26/2002	C1	winter	35	24.24	8.32	3.24	8.55	9.45	5.96	−1.59	0.65
11/26/2002	M1	winter	25	21.79	8.33	2.61	10.14	9.08	4.03	−0.67	0.53
02/18/2003	C1	winter	35	22.26	7.58	2.70	4.42	9.60	4.77	−0.05	0.80
02/18/2003	M2	winter	45	26.45	6.92	2.09	4.94	7.70	4.82	−1.95	0.81
03/06/2003	C1	upwelling	35	22.36	7.85	2.96	7.72	8.58	5.11	−1.43	0.65
03/06/2003	M1	upwelling	25	23.62	8.08	3.08	6.35	9.11	7.22	−3.12	0.73
03/06/2003	M2	upwelling	65	25.52	7.68	2.20	4.73	10.90	7.67	−2.25	0.81
03/27/2003	C1	upwelling	15	29.57	8.51	2.88	14.79	8.67	4.13	−1.08	0.50
03/27/2003	M1	upwelling	25	29.85	8.35	2.80	14.30	8.93	3.37	0.00	0.52
04/12/2003	C1	upwelling	25	24.20	7.75	3.20	4.53	7.80	3.61	−0.36	0.81
04/12/2003	M1	upwelling	35	28.06	7.70	3.71	10.34	7.89	3.24	0.66	0.63
06/24/2003	C1	upwelling	25	30.42	8.90	4.45	14.74	10.77	9.67	−3.36	0.52
06/24/2003	M1	upwelling	25	29.66	6.24	3.08	16.70	7.97	4.27	0.54	0.44
09/17/2003	C1	oceanic	15	25.02	7.74	3.56	7.40	7.42	6.71	−3.47	0.70
09/17/2003	M1	oceanic	15	23.66	7.24	3.81	6.91	6.18	9.52	−6.77	0.71
09/17/2003	M2	oceanic	15	28.36	6.96	3.38	2.02	8.67	19.01	−13.93	0.93
05/24/2004	C1	upwelling	25	30.45	5.93	1.75	13.84	6.18	4.18	−2.17	0.55
05/24/2004	M1	upwelling	25	31.05	7.24	3.66	16.37	8.03	3.15	1.30	0.47
05/24/2004	M2	upwelling	25	28.37	6.91	4.69	9.71	8.12	8.63	−2.73	0.66
06/15/2004	C1	upwelling	25	34.79	7.35	4.64	23.94	7.30	5.23	−0.65	0.31

[a]Values for f_n (see text) are calculated as 1 minus the surface concentration divided by the subsurface concentration. Dates are given as mm/dd/yyyy.
[b]Values of $\Delta(15,18)$ here are referenced to the subsurface water on the same sampling date (not mean North Pacific deep nitrate).

These values ranged from +5.9‰ to +8.9‰ for $\delta^{15}N$ and from +1.8‰ to +4.7‰ for $\delta^{18}O$ (Table 1) and are generally consistent with previous $\delta^{15}N_{NO3}$ data from Monterey Bay [*Altabet et al.*, 1999]. Deep water arriving in Monterey Bay via the California Countercurrent originates near the eastern edge of the North Pacific, where the simultaneous processes of N fixation and denitrification may give rise to negative values for $\Delta(15,18)$ as referenced to mean North Pacific deep water ($\delta^{15}N$ = +5‰ $\delta^{18}O$ = +3‰; (*Sigman et al.*, 2005)). Figures 2j, 2k, and 2l show profiles of $\Delta(15,18)$ when referenced to North Pacific deep water. In contrast to *Sigman et al.* [2005], the deep waters in our profiles exhibit positive values for $\Delta(15,18)$ ranging from +0.2‰ to +3.7‰, when referenced to mean North Pacific deep water (see discussion). Therefore, for the purposes of constraining euphotic zone nitrification, we choose to define $\Delta(15,18)$ in the euphotic zone as a deviation from the isotopic composition of NO_3^- directly below the mixed layer, rather than base the value of mean North Pacific data, in order to separate the localized phenomena within surface waters of Monterey Bay from those occurring in the greater eastern North Pacific.

[30] Figure 4 shows lines connecting the integrated NO_3^- isotopic composition of the deep water to that of the surface NO_3^- at each sampling date (Table 1). The 1:1 line is shown only for reference. Lines with slopes near 1 are indicative of isotopic compositions set largely by assimilation, while those with steeper slopes imply influence by nitrification occurring in euphotic zone. In most cases the lines trend upward with slopes steeper than 1, giving negative $\Delta(15,18)$ values, when referenced to the underlying water (see also trends in Figures 2j, 2k, and 2l).

5.2. Model Results

[31] For brevity, only the final expression resulting from combining the N and O mass balances to solve for $\Delta(15,18)$ is presented here (see aux. mat. for complete derivation). On the basis of the assumptions outlined above,

$$\Delta(15,18) = f_n * \left(\varepsilon_p - f_a * f_w * (\varepsilon_{ntr} - \varepsilon_a)\right) - \left(\frac{\delta^{18}O_{deep} - \delta^{18}O_{deep} * f_w + \left(\varepsilon_p * f_n\right) + \left(\delta^{18}O_{ntr} * f_n * f_w\right)}{1 - f_w + (f_n * f_w)}\right) + \delta^{18}O_{deep}, \quad (2)$$

where f_n is the fraction of NO_3^- drawdown in the surface water (based on NO_3^-concentration), f_a is the fraction of NH_4^+ that is reassimilated by phytoplankton, f_w is the fraction of NO_3^- assimilation supported by nitrification, $\delta^{18}O_{deep}$ is the $\delta^{18}O_{NO3}$ of subsurface water, $\delta^{18}O_{ntr}$ is the $\delta^{18}O$ resulting from nitrification. By using literature values to estimate isotope effects (ε_{ntr}, ε_a, and ε_p), this expression contains two unknowns, f_a and f_w.

[32] Before discussing the use of this model in Monterey Bay, it will be helpful to discuss some basic characteristics of the model and its sensitivity to certain parameters (Figure 5). The results of this model indicate that $\Delta(15,18)$ (the horizontal deviation from the expected line with a slope of 1:1) is directly related to the proportion of NO_3^- supplied by nitrification in the upper water column (f_w). Note that high values of f_w do not necessarily imply high rates of remineralization and/or nitrification. These values are strictly the proportion of NO_3^- in surface waters having originated from euphotic zone nitrification relative to that from upwelling. If the water column is well-stratified

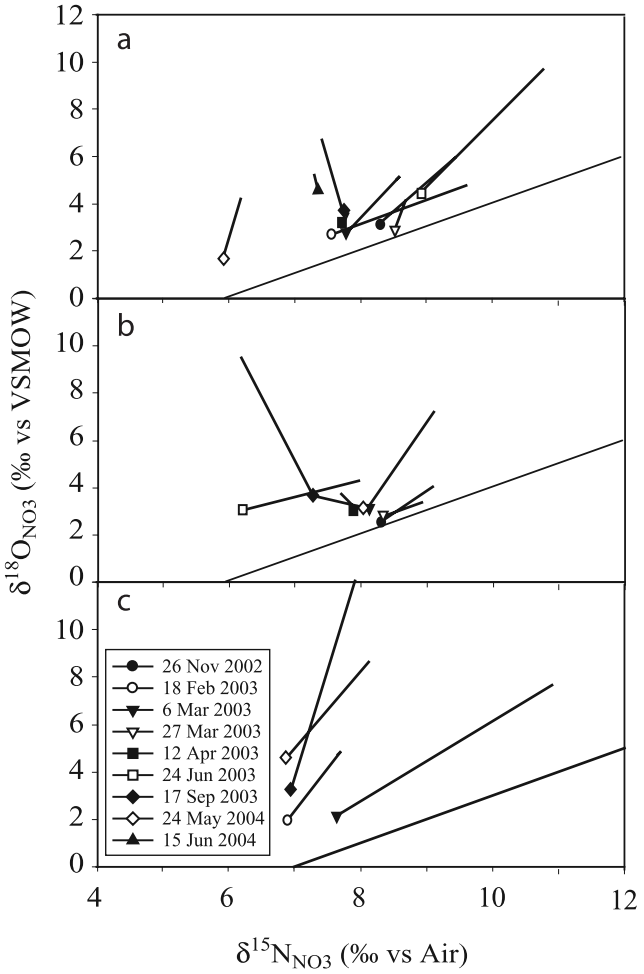

Figure 4. Plot illustrating differences between euphotic zone and subeuphotic zone NO_3^- isotopic composition at three sites in Monterey Bay (a) station C1, (b) station M1, and (c) station M2. Lines connect two points representing the deep water composition (symbol) and the surface water composition (no symbol). 1:1 line is shown only for reference. Note that where lines approximate a slope of 1, surface water NO_3^- isotopic composition is more strongly influenced by phytoplankton assimilation. Where slopes are steeper (>1) this is indicative of influence by surface NO_3^- regeneration.

and these waters have resided near the surface for relatively long periods, there will likely be a higher proportion of NO_3^- originating from nitrification even though rates may not be higher than during upwelling periods.

[33] As seen in equation (2), the use of $\Delta(15,18)$ to constrain values of f_w and f_a, is dependent on several variables, most of which were not directly characterized in this study. Particularly influential are the proportion of primary production which is remineralized in the surface water (f_r), the difference between the isotope effects for nitrification (ε_{ntr}) and NH_4^+ assimilation (ε_a), and the values used for both the $\delta^{18}O_{deep}$ (i.e., where the local reference line is based) and $\delta^{18}O_{ntr}$. The specific influence of these variables on estimates of euphotic zone nitrification and $\Delta(15,18)$ is discussed below.

5.2.1. Influence of Branching Between Ammonium Oxidation and Assimilation (f_a)

[34] To illustrate the influence of several of these variables, we plot modeled values for the NO_3^- dual isotopic composition for a given set of conditions, showing the effects of altering a single variable. Values for f_w and f_a are then unique for any point along each curve. First, Figure 5a shows how changes in ε_{ntr} (or more appropriately, the difference between ε_a and ε_{ntr}) influences $\Delta(15,18)$ when all other variables are held constant. With larger differences between ε_a and ε_{ntr}, the N directed back into the NO_3^- pool (and the NO_3^- pool itself) becomes lower in $\delta^{15}N$, causing $\Delta(15,18)$ to become more negative for a given amount of nitrification. Note that because branching ratios (f_a) of both 0 or 1 cause no net change to the $\delta^{15}N_{NO3}$, the curves described here begin and end at the same $\delta^{15}N_{NO3}$ values (yet still have different $\delta^{18}O_{NO3}$ values). For example, if all of the NH_4^+ generated during remineralization were simply reassimilated by phytoplankton ($f_a = 1$), then there is no nitrification and changes to $\delta^{15}N$ would be due to NO_3^- assimilation alone, with mass balance requiring no net change in $\delta^{15}N_{NO3}$. Conversely, if all of the N from remineralization were shuttled through nitrification ($f_a = 0$), mass balance would also dictate that the N returned to the NO_3^- pool would equal that of the PON pool, again resulting in no net change in $\delta^{15}N_{NO3}$.

[35] If ε_{ntr} and ε_a were equal, the isotopic composition of the N directed toward nitrification would be equal to that being recycled through phytoplankton with mass balance resulting in no net change to the $\delta^{15}N$ of the surface water NO_3^- pool. While the isotope effects for both processes are quite variable, values of ε_{ntr} (NH_4^+ oxidation) are generally thought to be much higher. *Casciotti et al.* [2002] determined that nitrifying bacteria can have ε_{ntr} values ranging from 14 to 38‰, with *Nitrosomonas marina*, a common marine nitrifier tending toward lower values between 14 and 19‰. The recent discovery of ammonium-oxidizing archaea (AOA) may also raise new questions about the role of archaea in N cycling [*Francis et al.*, 2005; *Könneke et al.*, 2005; *Schleper et al.*, 2005]. While we have no reason to suspect that N isotope effects for AOA will be different from those found in cultures of nitrifying bacteria, AOA have only recently been isolated in pure culture [*Könneke et al.*, 2005] and the isotope effects are still unknown. For NH_4^+ assimilation by phytoplankton, values of ε_a are also quite variable ranging from laboratory estimates of 19.6 ± 1‰ [*Waser et al.*, 1998] to field estimates of 6.5 to 9‰ [*Cifuentes et al.*, 1989; *Montoya et al.*, 1991]. *Pennock et al.* [1996] also estimated ε_a from laboratory experiments, showing a dependence on the NH_4^+ concentration causing values to range from 7.8‰ up to 27‰. Additionally, several of these studies suggested that at very low ambient NH_4^+ concentrations typical of ocean settings, these values, for both nitrifiers and phytoplankton, could be lower as diffusion of NH_4^+ into the cells becomes the rate limiting process. Unfortunately, very little data exist for ε_{ntr} or ε_a at low ambient NH_4^+ concentrations. Thus, for our purposes, we adopt a value for ε_{ntr} of 19‰ and for ε_a of 6‰. As mentioned, it is the difference between these values for nitrification and NH_4^+ assimilation that drives a low-$\delta^{15}N$

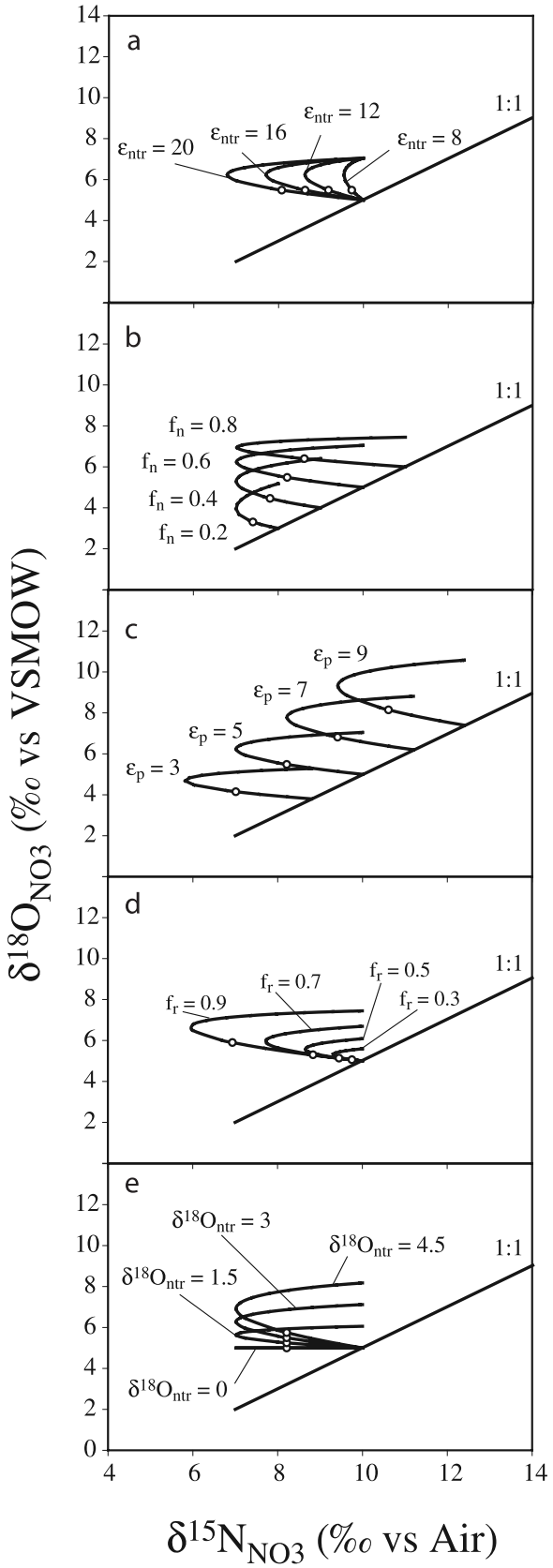

source of N back into the NO_3^- pool. Uncertainty in the values for these processes represents an unfortunate gap in our ability to model nitrification, and emphasizes the need for better understanding the isotopic discrimination inherent in these processes.

5.2.2. Influence of Drawdown (f_n), Nitrate Assimilation (ε_p), and Remineralization (f_r)

[36] Figure 5b shows how the magnitude of f_n influences $\Delta(15,18)$. As drawdown (f_n) increases, values of $\Delta(15,18)$ become more negative for a given proportion of NO_3^- supplied by nitrification (f_w), due to its larger relative contribution to a smaller NO_3^- pool. Interestingly, changes in ε_p, while playing an important role in determining the isotopic composition of NO_3^-, are only slightly linked to changes in $\Delta(15,18)$. As shown in Figure 5c, an increase in ε_p for a given set of conditions, causes $\delta^{15}N$ and $\delta^{18}O$ values to increase, but remain a similar distance from the reference line. In Figure 5d, as a greater proportion of primary productivity is remineralized (higher f_r), a given proportion of supply of NO_3^- by nitrification (f_w) is more influential on the NO_3^- pool resulting in more negative values of $\Delta(15,18)$.

5.2.3. Influence of $\delta^{18}O$ of Nitrification ($\delta^{18}O_{ntr}$)

[37] Changes in the value of $\delta^{18}O_{ntr}$ will also play a role in the estimation of nitrification using this approach. Figure 5e illustrates how, under the given conditions, various values for the $\delta^{18}O$ returning to the NO_3^- pool from nitrification influence NO_3^- isotopic composition. For higher values of $\delta^{18}O_{ntr}$, values of $\Delta(15,18)$ will also increase for the same amount of nitrification. Thus future research should also focus on the potential for variability in the oxygen isotope dynamics of nitrification.

5.2.4. Positive $\Delta(15,18)$ Values

[38] In fact, even positive values for $\Delta(15,18)$ are theoretically possible (Figure 6). For example, if isotopic discrimination were stronger for NH_4^+ assimilation than for nitrification ($\varepsilon_a > \varepsilon_{ntr}$), this would result in ^{15}N-enriched N being directed back into the N pool (still with no effect on $\delta^{18}O$). Thus accumulation of this ^{15}N-enriched N would result in higher $\delta^{15}N$ values, potentially leading to positive $\Delta(15,18)$ values with respect to the deeper water (Figure 6a). Likewise, if the value of $\delta^{18}O_{ntr}$ were actually lower than

Figure 5. Plot of modeled nitrate dual isotopic composition. Curved lines represent the range of nitrate isotopic composition with increased amounts of nitrification. The intersection of these curves with the 1:1 line represents no nitrification while the end represents a hypothetical maximum proportion of nitrate stemming from nitrification (~99%). White circles indicate isotopic composition at which 25% of nitrate uptake is supplied by nitrification (f_w = 0.25). For all plots, the model parameters are: f_n = 0.6 (i.e., 60% drawdown by phytoplankton), ε_p = 5‰, ε_{ntr} = 19‰, ε_a = 6‰, f_a = 0.67, and $\delta^{18}O_{ntr}$ = +2.9‰, unless otherwise noted. (a) Effects of various values for fractionation during nitrification (ε_{ntr}), (b) effects of various values of f_n, (c) effects of various values of ε_p, (d) effects of various values of f_r, and (e) effects of various values of $\delta^{18}O_{ntr}$.

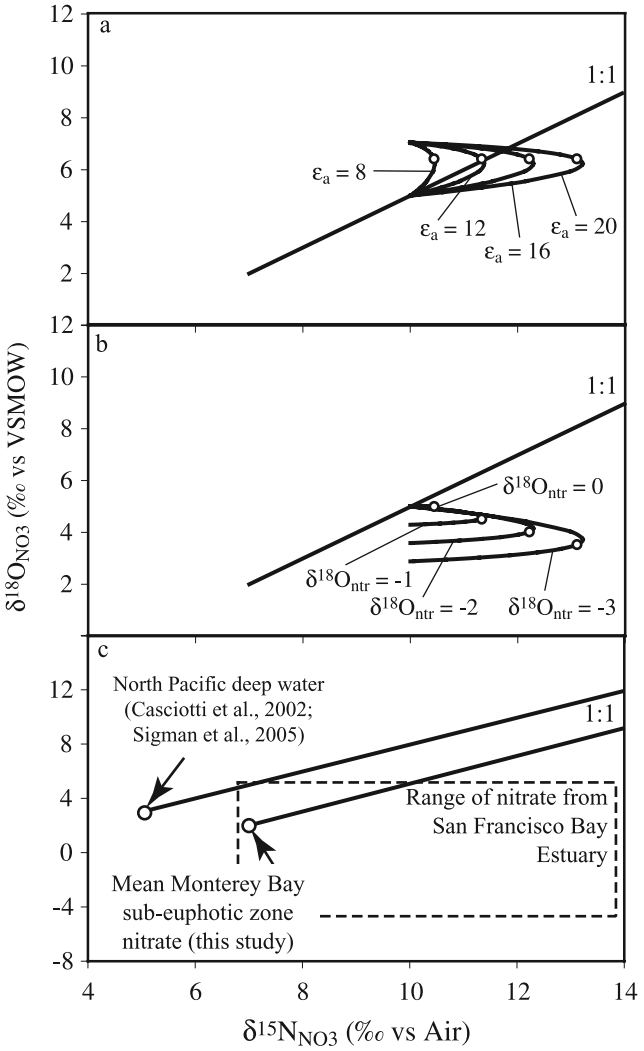

Figure 6. Plot of modeled nitrate isotopic composition illustrating conditions under which positive values of $\Delta(15,18)$ could occur. 1:1 line originates at a hypothetical deep water nitrate composition typical of Monterey Bay ($\delta^{15}N$ = +7‰, $\delta^{18}O$ = +2‰). (a) Effects of variation in values of ε_a when they exceed those of ε_{ntr}. Model parameters are: ε_{ntr} = 6‰, ε_p = 5‰, f_a = 0.67, f_n = 0.6, and $\delta^{18}O_{ntr}$ = 2.9‰. (b) Effects of values for $\delta^{18}O_{ntr}$ when $<\delta^{18}O_{deep}$; otherwise they are the same as in Figure 6a. (c) Difference between mean nitrate composition in North Pacific deep water, Monterey Bay at 200 m and the San Francisco Bay estuary just north of Monterey Bay.

$\delta^{18}O_{deep}$, (e.g., 0‰ instead of 3‰) then ^{18}O-depleted O would be directed back into the surface NO_3^- pool, and would exaggerate this effect also resulting in positive $\Delta(15,18)$ values (Figure 6b). From this, it follows that there could be a hypothetical input $\delta^{18}O_{NO3}$ value for which a nitrification signal will not be expressed at all, despite its presence.

[39] Finally, if significant inputs of terrestrial (riverine or estuarine) N were to influence NO_3^- isotopic composition along coastal margins, this could also impact the $\Delta(15,18)$ observed in surface waters relative to underlying deeper, less influenced water. NO_3^- in San Francisco Bay just north of Monterey Bay, for example, was shown to have $\delta^{15}N$ values of +7 to +14‰ and $\delta^{18}O$ values from −6 to +4‰ (albeit during the drier summer months) [*Wankel et al.*, 2006]. These values would also potentially influence $\Delta(15,18)$ values, since San Francisco Bay has $\Delta(15,18)$ values ranging from +0.5 to +12 relative to mean North Pacific deep water (Figure 6c). While this is perhaps not an entirely meaningful comparison, it serves to illustrate that such an influence could be important on a regional scale, especially along coastal margins.

[40] The NO_3- dual isotopic composition modeled with values for f_r, ε_a, ε_{ntr} and ε_p that fit a hypothetical surface water composition representative of Monterey Bay surface water ($\delta^{15}N$ = +10.9‰; $\delta^{18}O$ = +7.0‰) and deep water ($\delta^{15}N$ = +7‰; $\delta^{18}O$ = +2‰) is shown in Figure 7 illustrating how multiple solutions can exist for a given NO_3^- isotopic composition when f_r, ε_a, ε_{ntr} and/or ε_p are poorly constrained.

5.3. Results of Model Fitting

[41] Values for $\Delta(15,18)$ in surface water relative to deep water observed in Monterey Bay suggest the cooccurrence of NO_3^- assimilation and nitrification. Calculated values of $\Delta(15,18)$ for the integrated surface box range from −13.9‰ to +1.3‰ (Table 2) also suggesting a high degree of variability in the biogeochemical processes occurring in surface waters of Monterey Bay.

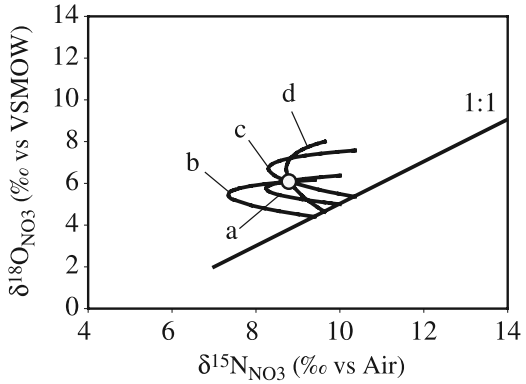

Figure 7. Plot of NO_3^- dual isotopic composition modeled with various values for f_r, ε_{ntr}, ε_p and ε_a, fitting a hypothetical surface water composition (white circle, $\delta^{15}N$ = +8.8‰; $\delta^{18}O$ = +6.1‰) relative to a deep water composition ($\delta^{15}N$ = +7‰; $\delta^{18}O$ = +2‰). A hypothetical value of 0.6 is assumed for f_n (i.e., 60% drawdown by phytoplankton; surface water has 60% less nitrate than deep). Plot illustrates that multiple solutions are possible for any dual isotopic composition (and value of $\Delta(15,18)$) when values of f_r, ε_p, ε_a and ε_{ntr} are poorly constrained. Curved lines represent different unique solutions for various proportions of NO_3^- uptake supported by nitrification. Line a, ε_a = 6.0‰, ε_{ntr} = 15‰, f_r = 0.8, ε_p = 4.0‰; line b, ε_a = 6.0‰, ε_{ntr} = 19‰, f_r = 0.6, ε_p = 5.0‰; line c, ε_a = 6.0‰, ε_{ntr} = 10‰, f_r = 0.8, ε_p = 4.4‰; and line d, ε_a = 6.0‰, ε_{ntr} = 15‰, f_r = 0.8, ε_p = 5.6‰.

Table 2. Results of Model Fitting of Monterey Bay Nitrate Isotope Data[a]

		f_w			f ratio			f_a			ε_p			$\delta^{15}N_{PON}$		
Date	Site	f_r 0.8	f_r 0.5	Mid	f_r 0.8	f_r 0.5	Mid	f_r 0.8	f_r 0.5	Mid	f_r 0.8	f_r 0.5	Mid	f_r 0.8	f_r 0.5	Mid
11/26/2002	C1	0.18	0.25	0.22	0.24	0.67	0.46	0.94	0.67	0.81	4.0	3.9	4.0	8.8	10.2	9.5
11/26/2002	M1	0.09	0.10	0.10	0.22	0.55	0.39	0.98	0.89	0.94	2.5	2.5	2.5	8.1	8.3	8.2
02/18/2003	C1	0.01	0.01	0.01	0.20	0.20	0.20	0.99	0.99	0.99	2.6	2.6	2.6	7.1	7.1	7.1
02/18/2003	M2	0.18	0.22	0.20	0.24	0.65	0.45	0.95	0.71	0.83	3.1	3.0	3.1	7.8	8.8	8.3
03/06/2003	C1	0.17	0.20	0.19	0.24	0.63	0.44	0.95	0.74	0.85	3.2	3.1	3.1	8.4	9.2	8.8
03/06/2003	M1	0.34			0.30			0.87			5.2			10.0		
03/06/2003	M2	0.20	0.28	0.24	0.25	0.69	0.47	0.94	0.62	0.78	6.3	6.2	6.3	8.1	9.3	8.7
03/27/2003	C1	0.16	0.20	0.18	0.24	0.62	0.43	0.95	0.76	0.86	2.3	2.3	2.3	9.2	10.0	9.6
03/27/2003	M1	0.00	0.00	0.00	0.20	0.20	0.20	1.00	1.00	1.00	1.1	1.1	1.1	7.8	7.8	7.8
04/12/2003	C1	0.03	0.04	0.04	0.21	0.52	0.37	0.99	0.96	0.98	0.5	0.5	0.5	7.9	7.9	7.9
04/12/2003	M1															
06/24/2003	C1	0.49			0.40			0.76			8.5			11.3		
06/24/2003	M1															
09/17/2003	C1	0.45			0.36			0.80			4.2			11.4		
09/17/2003	M1															
09/17/2003	M2															
05/24/2004	C1	0.26			0.27			0.91			3.6			7.4		
05/24/2004	M1															
05/24/2004	M2	0.37			0.32			0.86			5.9			8.8		
06/15/2004	C1	0.18	0.26	0.22	0.24	0.67	0.46	0.95	0.65	0.80	2.0	2.0	2.0	8.4	10.0	9.2

[a]Parameters listed are calculated on the basis of assumptions listed in the text. Calculated values are shown for f_w, f-ratio, f_a, and ε_p, using a value of either 0.5 or 0.8 for f_r [*Pennington et al.*, 2007]. Dates are given as mm/dd/yyyy. No entry denotes no possible model solution based on boundary conditions outlined in the text.

[42] We use the observed values for both deep and surface water $\delta^{15}N_{NO3}$, $\delta^{18}O_{NO3}$ (i.e., $\Delta(15,18)$) and NO_3^- concentrations in connection with values found in the literature for ε_a (6‰ [*Cifuentes et al.*, 1989; *Montoya et al.*, 1991; *Waser et al.*, 1998]) and ε_{ntr} (19‰ [*Casciotti et al.*, 2003]), as well as a range of values of f_r (0.5 to 0.8) specific to Monterey Bay [*Pennington et al.*, 2007] to estimate the proportion of nitrate-supported primary productivity that is supplied through nitrification (f_w). The range of values of f_r found in *Pennington et al.* [2007] allowed us to solve equation (2) and estimate minimum and maximum values for f_a and f_w. Furthermore, although technically two unique solutions are possible (see curves in Figure 5), only one solution coincides with $\delta^{15}N_{PON}$ values which are reasonable (+1 to +9 [*Rau et al.*, 1998]). For a given value of f_r, we report calculated values for f_a, f_w, as well as the 'true' f ratio (NO_3^- assim/NO_3^- + NH_4^+ assim), and values for ε_p (Table 2).

[43] Solutions were found for most profiles and we present here results for the model solutions only for cases where solutions were possible (reasons for not getting viable solutions are discussed below). Model-predicted values for ε_p range from a minimum of 0.5‰ to a maximum of 8.5‰ (Table 2), and are within the range of published values [*Granger et al.*, 2004]. Values for ε_p at stations C1 and M1 averaged ~3.4 and ~3.0‰, respectively, while those for M2 (most offshore) are higher (~5.1‰), though not significantly. Many field calculated values for ε_p are based on shipboard incubations or simultaneous measurements of $\delta^{15}N_{NO3}$ and NO_3^- concentrations in the water column [e.g., *Altabet et al.*, 1999, and references therein] and thus might be affected by nitrification. For example, if we calculate ε_p values using only changes in $\delta^{15}N_{NO3}$ and NO_3^- concentrations (data not shown), the values are generally lower than those calculated using our model to constrain ε_p.

5.3.1. Model-Predicted $\delta^{15}N_{PON}$

[44] Predicted values for surface $\delta^{15}N_{PON}$ range from +7.1 to +11.4‰ (Table 2) with average values of +9.1 ± 1.5, +8.7 ± 1.1, and +8.6 ± 0.3‰ for stations C1, M1 and M2, respectively; however, differences were not statistically different. These are consistent with sediment trap data from Monterey Bay [*Altabet et al.*, 1999; S. D. Wankel and A. Paytan, unpublished data, 2005]; however, they are higher than those typically observed suspended in surface waters [*Rau et al.*, 1998]. Fractionation during export of PON was not explicitly addressed in this study, the exclusion of which may be an oversimplification in our modeling approach.

[45] Notably, in this model $\delta^{15}N_{pon}$ values are influenced by the relative amount of surface water nitrification (f_w), the branching ratio (f_a), as well as the difference between ε_{ntr} and ε_a. For example, at steady state if $\varepsilon_{ntr} \gg \varepsilon_a$, then nitrification drives lower $\delta^{15}N$ values into the NO_3^- pool while causing $\delta^{15}N_{pon}$ values to increase. If we assume no fractionation by remineralization during sinking, then in this scenario, compared to one with no surface nitrification, the $\delta^{15}N$ of exported PON would be higher. If the influence of nitrification were found to be variable over large spatial and/or temporal scales, then nitrification might play an important role in the paleoceanographic record of $\delta^{15}N_{pon}$ as others have suggested [*Sutka et al.*, 2004], and caution should be exercised when using $\delta^{15}N_{pon}$ data to reconstruct NO_3^- utilization [*Altabet and Francois*, 1994; *Ganeshram et al.*, 2000].

5.3.2. Nitrification (f_w)

[46] Model calculated values for f_w, the fraction of NO_3^- assimilation supported by nitrification, ranged from 0 to 0.49. These values are proportional (though not linearly) to the overestimation of the f ratio, caused by the presence of surface water nitrification. Mean values for C1, M1 and M2 were 0.23 ± 0.16, 0.15 ± 0.18 and 0.27 ± 0.09, respectively,

indicating that on average ~15–27% of NO_3^- assimilation in surface waters in Monterey Bay is supported by nitrification. Mean f ratios calculated for C1, M1 and M2, were 0.37 ± 0.09, 0.30 ± 0.09 and 0.41 ± 0.08, respectively. Other estimates of f ratios in this region are higher (0.84 [*Olivieri and Chavez*, 2000]; 0.49 [*Pennington et al.*, 2007]) but are perhaps underestimating the amount of productivity supported by nitrification.

5.3.3. NH_4^+ Oxidation (f_a)

[47] Values for f_a, the fraction of regenerated NH_4^+ that is shuttled toward phytoplankton assimilation (rather than nitrification), ranged from 0.67 to 0.95, with mean values at C1, M1 and M2 of 0.86 ± 0.08, 0.94 ± 0.06 and 0.82 ± 0.04, respectively, with M1 significantly different from M2 ($p = 0.044$). This suggests that while most of the NH_4^+ is utilized by phytoplankton, there is nevertheless an important fraction supporting nitrification within the surface layer. Indeed, using a ^{15}N tracer approach, *Ward* [2005] showed even lower values for f_a (0.67 to 0.79) indicative of significant amounts of nitrification. Thus the findings here independently support those of *Ward* [2005] and argue for ubiquitous nitrification occurring in the surface ocean.

5.3.4. f_w Versus ε_p

[48] Notably, there is a positive correlation between the model-predicted values of f_w and ε_p ($r^2 = 0.65$; $p < 0.001$; data not shown). There are at least two potential explanations for this relationship. The first may exist due to the effect of substrate availability on the expression of fractionations. When a substrate is abundant, there will often be a more pronounced expression of isotopic discrimination or larger values of ε. In the case of phytoplankton, increased supply of NO_3^- by nitrification may partially relieve the immediate growth demand, perhaps leading to a higher intracellular NO_3^- efflux and a larger external expression of the internal fractionation [*Needoba et al.*, 2004]. If true, this phenomenon suggests that while there may be a decoupling of hydrographic and biogeochemical signals [*Altabet et al.*, 1999; *Ward*, 2005], coupled N and O isotopes offer a tool for improving constraints on N cycling.

[49] A second explanation could be the variable influence of light on phytoplankton and nitrifying bacteria. At deeper depths in the surface layer (less light), nitrifying bacteria may more successfully compete with phytoplankton for NH_4^+ leading to higher values for f_w (i.e., more NH_4^+ going to nitrification). Additionally, under light limiting growth conditions, phytoplankton may exhibit increased fractionation [*Needoba et al.*, 2004], thus potentially leading to a correlation between f_w and ε_p.

5.3.5. No Solutions

[50] For both models there were several dates for which no solution could be found using the outlined parameters. For three sampling dates at M1 (12 April 2003, 24 June 2003, and 24 May 2004) positive values for $\Delta(15,18)$ were found. As mentioned above, these could potentially be explained by cycling mechanisms in which ε_a exceeds ε_{ntr} and/or in which $\delta^{18}O_{ntr} < \delta^{18}O_{deep}$. This emphasizes the need for a better understanding of the controls on $\delta^{18}O_{ntr}$ as well as the interplay between isotopic fractionation of nitrification and NH_4^+ assimilation and the branching ratio between them.

[51] Finally, there was only one cruise during the late summer, or 'oceanic' season of Monterey Bay (17 September 2003). Profiles from all three sites on this date showed markedly different NO_3^- isotope patterns. At all three sites $\delta^{15}N_{NO3}$ decrease in surface waters with respect to deep water, potentially explainable through inputs by N fixation which might be observed during this period and/or a situation in which $\varepsilon_{ntr} \gg \varepsilon_a$. However, these lower $\delta^{15}N_{NO3}$ values also coincide with very high $\delta^{18}O$ values (up to +34‰) which are not expected from the above processes. Moreover, in these cases, the mixed layer is relatively shallow (15 m), the integrated surface water NO_3^- concentrations are generally low (2 to 7 μM) and thus f_n is high (0.70 to 0.93). In this case, the high $\Delta(15,18)$ values may suggest the influence of inputs of atmospheric NO_3^-. Atmospheric NO_3^- has very high $\delta^{18}O$ values (+65 to +90‰) and a relatively low $\delta^{15}N$ value (−12 to +2‰) [*Kendall*, 1998; *Hastings et al.*, 2003]. Therefore atmospheric NO_3^-, which is unaccounted for in this model, could increase $\delta^{18}O_{NO3}$ values and lower $\delta^{15}N_{NO3}$ values in the surface box, rendering an estimation of nitrification with this approach incorrect.

[52] In more extreme cases, no solution will exist, as is the case for M2 (17 September 2003) when $\Delta(15,18)$ was −13.9‰. Station M2 is routinely the most stratified and least influenced by upwelling [*Kudela and Chavez*, 2000; *Pennington and Chavez*, 2000; *Kudela and Chavez*, 2002]. In fact, M2 regularly had the highest values for $\delta^{15}N_{NO3}$ and $\delta^{18}O_{NO3}$, partially due to the more stratified nature and larger proportion of NO_3^- drawdown relative to the input from underlying waters (Figures 2 and 3). Thus, while surface waters at C1 and M1 may be more influenced by an upwelling isotopic composition, the nature of surface water at M2 implies a longer residence time allowing for a potentially more protracted influence by atmospheric deposition. While we cannot unequivocally demonstrate influence by atmospheric NO_3^- deposition in the surface waters of Monterey Bay using data presented here, preliminary data support the existence of positive $\Delta^{17}O_{NO3}$ values in surface waters of Monterey Bay (S. D. Wankel, unpublished data, 2005) supporting the influence of atmospheric source [*Michalski et al.*, 2003]. Future work is needed to verify this potential impact and provide a more definitive perspective on the importance of atmospheric deposition to surface waters.

6. Conclusions

[53] We show that NO_3^- dual isotopic composition can be used to improve our understanding of the complexity of the marine N cycle in the euphotic zone. Using coupled measurements of $\delta^{15}N_{NO3}$ and $\delta^{18}O_{NO3}$ we show that euphotic zone nitrification plays a previously unrecognized and substantial role in the gross productivity in Monterey Bay ultimately supporting on average ~30% of total NO_3^- based production. Failure to include this recycled NO_3^- production may grossly underestimate regenerated production and overestimate f ratios. Furthermore, this implies a more significant role for euphotic zone nitrification in regulating primary productivity.

[54] On the basis of the modeling results, it is clear that the branching between nitrification and phytoplankton NH_4^+

assimilation exerts a strong control on surface NO_3^- isotopic composition. Our modeling indicates that ultimately it may prove most difficult to adequately constrain values for ε_{ntr}, and ε_a, and emphasizes the need for a better understanding of both processes. Furthermore, in highly dynamic settings, such as Monterey Bay, it may be even more difficult to constrain these processes given the relatively small and highly variable temporal and spatial scales of many of the hydrodynamic processes operating. Nonetheless, coupled N and O isotopes of NO_3^- offer a unique means for estimating some of the combined effects of N cycling processes.

[55] This method for evaluating upper water column N cycling, while promising, is still in its infancy. However, there exists the strong potential of combining this approach, as well as measurements of $\delta^{15}N_{PON}$, with simultaneous measurements of photosynthetic rates (^{14}C incubations) and nitrification rates (^{15}N incubations) in order to better constrain the role of nitrification within the euphotic zone in supporting upper water column productivity. Furthermore, linking dual isotopic measurements of NO_3^- (and ultimately NO_2^-) with modern molecular approaches (e.g., gene expression by the nitrifying community) will allow a better understanding of the functioning and complexity of microbial nitrogen cycling in aquatic systems.

[56] **Acknowledgments.** This work was supported in part by a NOAA National Estuarine Research Reserve–Elkhorn Slough graduate fellowship to S. D. W., an NSF grant (ECS-0308070) to A. P., the USGS National Research Program for C. K., and the Lucille and David Packard Foundation for J. T. P. and F. P. C. Development of this manuscript benefited significantly from helpful discussions with Julie Granger, Daniel Sigman, Karen Casciotti, Alessandro Tagliabue, Curtis Deutsch, Dan Doctor, and Steve Silva. Enlightening reviews by Daniel Sigman and Karen Casciotti also greatly helped to improve this manuscript. CTD and nutrient data were graciously measured and provided by MBARI. The authors would like to thank Karen McLaughlin and David Nicholson for their assistance with sample collection. We would also like to thank the Captain and crew of the R/V *Point Lobos* for providing safe transport and technical support in Monterey Bay.

References

Altabet, M. A., and R. Francois (1994), Sedimentary nitrogen isotopic ratio as a recorder for surface ocean nitrate utilization, *Global Biogeochem. Cycles*, *8*(1), 103–116.

Altabet, M. A., C. Pilskaln, R. C. Thunell, C. Pride, D. M. Sigman, F. P. Chavez, and R. Francois (1999), The nitrogen isotope biogeochemistry of sinking particles from the margin of the eastern North Pacific, *Deep Sea Res., Part I*, *46*, 655–679.

Andersson, K. K., and A. B. Hooper (1983), O_2 and H_2O are each the source of one O in NO_2 produced from NH_3 by Nitrosomonas: ^{15}N-NMR evidence, *FEBS Lett.*, *164*, 236–240.

Andersson, K. K., S. B. Philson, and A. B. Hooper (1982), ^{18}O isotope shift in ^{15}N NMR analysis of biological N-oxidations: H_2O-NO_2- exchange in the ammonia-oxidizing bacterium Nitrosomonas, *Proc. Natl. Acad. Sci. U. S. A.*, *79*, 5871–5875.

Bianchi, M., F. Feliatra, P. Treguer, M.-A. Vincendeau, and J. Morvan (1997), Nitrification rates, ammonium and nitrate distribution in upper layers of the water column and in sediments of the Indian sector of the Southern Ocean, *Deep Sea Res., Part II*, *44*, 1017–1032.

Böhlke, J., S. Mroczkowski, and T. B. Coplen (2003), Oxygen isotopes in nitrate: New reference materials for ^{18}O:^{17}O:^{16}O measurements and observations on nitrate-water equilibration, *Rapid Commun. Mass Spectrom.*, *17*, 1835–1846.

Brandes, J. A., and A. H. Devol (2002), A global marine-fixed nitrogen isotopic budget: Implications for Holocene nitrogen cycling, *Global Biogeochem. Cycles*, *16*(4), 1120, doi:10.1029/2001GB001856.

Breaker, L. C., and W. W. Broenkow (1994), The circulation of Monterey Bay and related processes, *Oceanogr. Mar. Biol.*, *32*, 1–64.

Casciotti, K. L., D. M. Sigman, M. Galanter-Hastings, J. K. Böhlke, and A. Hilkert (2002), A bacterial method for the measurement of the oxygen isotope composition in marine and fresh waters, *Anal. Chem.*, *74*, 4905–4912.

Casciotti, K. L., D. M. Sigman, and B. B. Ward (2003), Linking diversity and stable isotope fractionation in ammonia-oxidizing bacteria, *Geomicrobiol. J.*, *20*, 335–353.

Chavez, F. P. (1995), A comparison of ship and satellite chlorophyll from California and Peru, *J. Geophys. Res.*, *100*, 24,855–24,862.

Chavez, F. P. (1996), Forcing and biological impact of onset of the 1992 El Niño in central California, *Geophys. Res. Lett.*, *23*, 265–268.

Checkley, D. M., Jr., and C. A. Miller (1989), Nitrogen isotope fractionation by oceanic zooplankton, *Deep Sea Res.*, *36*, 1449–1456.

Cifuentes, L. A., M. F. Fogel, and J. R. Pennock (1989), Biogeochemical factors that influence the stable nitrogen isotope ratio of dissolved ammonium in the Delaware estuary, *Geochim. Cosmochim. Acta*, *53*, 2713–2721.

Dore, J. E., and D. M. Karl (1996), Nitrification in the euphotic zone as a source of nitrite, nitrate, and nitrous oxide at Station ALOHA, *Limnol. Oceanogr.*, *41*(8), 1619–1628.

Dugdale, R. C., and J. J. Goering (1967), Uptake of new and regenerated forms of nitrogen in primary productivity, *Limnol. Oceanogr.*, *12*(2), 196–206.

Eppley, R. W., and B. J. Peterson (1979), Particulate organic matter flux and planktonic new production in the deep ocean, *Nature*, *282*, 677–680.

Francis, C. A., K. J. Roberts, J. M. Beman, A. E. Santoro, and B. B. Oakley (2005), Ubiquity and diversity of ammonia-oxidizing archaea in water columns and sediments of the ocean, *Proc. Natl. Acad. Sci. U. S. A.*, *102*, 14,683–14,688.

Ganeshram, R. S., T. F. Pedersen, S. E. Calvert, G. W. McNeill, and M. R. Fontugne (2000), Glacial-interglacial variability in denitrification in the world's oceans: Causes and consequences, *Paleoceanography*, *15*(4), 361–376.

Granger, J. (2006), Coupled measurements of the $\delta^{15}N$ and the $\delta^{18}O$ of nitrate as tracers for ocean nitrogen processes, Ph.D. thesis, Univ. of B. C., Vancouver, British Columbia, Canada.

Granger, J., D. M. Sigman, J. A. Needoba, and P. J. Harrison (2004), Coupled nitrogen and oxygen isotope fractionation of nitrate during assimilation by cultures of marine phytoplankton, *Limnol. Oceanogr.*, *49*(5), 1763–1773.

Hastings, M. G., D. M. Sigman, and F. Lipschultz (2003), Isotopic evidence for source changes of nitrate in rain at Bermuda, *J. Geophys. Res.*, *108*(D24), 4790, doi:10.1029/2003JD003789.

Hoch, M. P., M. F. Fogel, and D. L. Kirchman (1992), Isotope fractionation associated with ammonium uptake by a marine bacterium, *Limnol. Oceanogr.*, *37*(7), 1447–1459.

Hollocher, T. C. (1984), Source of the oxygen atoms of nitrate in the oxidation of nitrite by Nitrobacter agilis and evidence against a P-O-N anhydride mechanism in oxidative phosphorylation, *Arch. Biochem. Biophys.*, *233*(2), 721–727.

Karl, D. M., and A. F. Michaels (2001), Nitrogen cycle, in *Encylopedia of Ocean Science,* edited by J. H. Steele et al., pp. 1876–1884, Elsevier, New York.

Kendall, C. (1998), *Isotope Tracers in Catchment Hydrology*, Elsevier, New York.

Könneke, M., A. E. Bernhard, J. de la Torre, C. B. Walker, J. B. Waterbury, and D. A. Stahl (2005), Isolation of an autotrophic ammonia oxidizing marine archeon, *Nature*, *437*, 543–546.

Kudela, R. M., and F. P. Chavez (2000), Modeling the impact of the 1992 El Niño on new production in Monterey Bay, California, *Deep Sea Res., Part II*, *47*, 1055–1076.

Kudela, R. M., and F. P. Chavez (2002), Multi-platform remote sensing of new production in central California during the 1997–1998 El Niño, *Prog. Oceanogr.*, *54*, 233–249.

Kudela, R. M., and R. C. Dugdale (2000), Nutrient regulation of phytoplankton productivity in Monterey Bay, California, *Deep Sea Res., Part II*, *47*, 1023–1053.

Kumar, S., D. J. D. Nicholas, and E. H. Williams (1983), Definitive ^{15}N NMR evidence that water serves as a source of O during nitrite oxidation by Nitrobacter agilis, *FEBS Lett.*, *152*, 71–74.

Lehmann, M. F., D. M. Sigman, and W. M. Berelson (2004), Coupling the $^{15}N/^{14}N$ and $^{18}O/^{16}O$ of nitrate as a constraint on benthic nitrogen cycling, *Mar. Chem.*, *88*, 1–20.

Michalski, G., Z. Scott, M. Kabiling, and M. H. Thiemens (2003), First measurements and modeling of $\Delta^{17}O$ in atmospheric nitrate, *Geophys. Res. Lett.*, *30*(16), 1870, doi:10.1029/2003GL017015.

Montoya, J. P., S. G. Korrigan, and J. J. McCarthy (1991), Rapid, storm-induced changes in the natural abundance of ^{15}N in a planktonic ecosystem, Chesapeake Bay, USA, *Geochim. Cosmochim. Acta*, *55*, 3627–3638.

Needoba, J. A., D. M. Sigman, and P. J. Harrison (2004), The mechanism of isotope fractionation during algal nitrate assimilation as illuminated by the $^{15}N/^{14}N$ of intracellular nitrate, *J. Phycol.*, *40*, 517–522.

Olivieri, R. A., and F. P. Chavez (2000), A model of plankton dynamics for the coastal upwelling system of Monterey Bay, *Deep Sea Res., Part II*, *47*, 1077–1106.

Pennington, J. T., and F. P. Chavez (2000), Seasonal fluctuations of temperature, salinity, nitrate, chlorophyll and primary production at station H3/M1 over 1989–1996 in Monterey Bay, California, *Deep Sea Res., Part II*, *47*, 947–973.

Pennington, J. T., G. E. Friederich, G. C. Castro, C. A. Collins, W. W. Evans, and F. P. Chavez (2007), A carbon budget for the northern and central California coastal upwelling system, in *Continental Margins Task Team, The Synthesis Book*, Springer, New York, in press.

Pennock, J., D. Velinsky, J. Ludlam, J. Sharp, and M. Fogel (1996), Isotopic fractionation of ammonium and nitrate during uptake by Skeletonema costatum: Implications for $\delta^{15}N$ dynamics under bloom conditions, *Limnol. Oceanogr.*, *41*(3), 451–459.

Raimbault, P., G. Slawyk, B. Boudejellal, C. Coatanoan, P. Conan, B. Coste, N. Garcia, T. Moutin, and M. Pujo-Pay (1999), Carbon and nitrogen uptake and export in the equatorial Pacific at 150W: Evidence of an efficient regenerated production cycle, *J. Geophys. Res.*, *104*(C2), 3341–3356.

Rau, G., C. Low, J. T. Pennington, K. R. Buck, and F. P. Chavez (1998), Suspended particulate nitrogen $d^{15}N$ versus nitrate utilization: Observations from Monterey Bay, CA, *Deep Sea Res., Part II*, *45*, 1603–1616.

Sarmiento, J. L., R. D. Slater, J. R. Toggweiler, M. J. R. Fasham, H. Ducklow, and G. T. Evans (1993), A seasonal three-dimensional ecosystem model of nitrogen cycling in the North Atlantic euphotic zone, *Global Biogeochem. Cycles*, *7*, 417–450.

Schleper, C., G. Jürgens, and M. Jonuscheit (2005), Genomic studies of uncultivated archaea, *Nature Rev. Microbiol.*, *3*, 479–488.

Sigman, D. M., and K. L. Casciotti (2001), Nitrogen isotopes in the ocean, in *Encyclopedia of Ocean Sciences,* edited by J. H. Steele et al., pp. 1884–1894, Elsevier, New York.

Sigman, D. M., K. L. Casciotti, M. Andreani, C. Barford, M. Galanter, and J. K. Böhlke (2001), A bacterial method for the nitrogen isotopic analysis of nitrate in seawater and freshwater, *Anal. Chem.*, *73*, 4145–4153.

Sigman, D. M., R. Robinson, A. N. Knapp, A. van Geen, D. C. McCorkle, J. A. Brandes, and R. C. Thunell (2003), Distinguishing between water column and sedimentary denitrification in the Santa Barbara Basin using the stable isotopes of nitrate, *Geochem. Geophys. Geosyst.*, *4*(5), 1040, doi:10.1029/2002GC000384.

Sigman, D. M., J. Granger, P. J. DiFiore, M. M. Lehmann, R. Ho, G. Cane, and A. van Geen (2005), Coupled nitrogen and oxygen isotope measurements of nitrate along the eastern North Pacific margin, *Global Biogeochem. Cycles*, *19*, GB4022, doi:10.1029/2005GB002458.

Sutka, R. L., N. E. Ostrom, P. H. Ostrom, and M. S. Phanikumar (2004), Stable nitrogen isotope dynamics of dissolved nitrate in a transect from the North Pacific Subtropical Gyre to the Eastern Tropical North Pacific, *Geochim. Cosmochim. Acta*, *68*, 517–527.

Wankel, S. D., C. Kendall, C. A. Francis, and A. Paytan (2006), Nitrogen sources and cycling in the San Francisco Bay Estuary: A nitrate dual isotopic composition approach, *Limnol. Oceanogr.*, *51*(4), 1654–1664.

Ward, B. B. (2005), Temporal variability in nitrification rates and related biogeochemical factors in Monterey Bay, California, USA, *Mar. Ecol. Prog. Ser.*, *292*, 97–109.

Ward, B. B., K. A. Kilpatrick, E. H. Renger, and R. W. Eppley (1989), Biological nitrogen cycling in the nitracline, *Limnol. Oceanogr.*, *34*(3), 493–513.

Waser, N. A. D., P. J. Harrison, B. Nielsen, and H. E. Calvert (1998), Nitrogen isotope fractionation during the uptake and assimilation of nitrate, nitrite, ammonium and urea by a marine diatom, *Limnol. Oceanogr.*, *43*(2), 215–224.

F. P. Chavez and J. T. Pennington, Monterey Bay Aquarium Research Institute, 700 Sandholdt Road, Moss Landing, CA 95039, USA.

C. Kendall, United States Geological Survey, 345 Middlefield Rd., MS 434, Menlo Park, CA 94025, USA.

A. Paytan, Department of Geological and Environmental Sciences, Stanford University, 320 Braun Hall, Stanford, CA 94305, USA.

S. Wankel, Department of Organismal and Evolutionary Biology, Harvard University, 16 Divinity Avenue, Room 3092, Cambridge, MA 02138, USA. (swankel@oeb.harvard.edu)